Pergamon

Cement and Concrete Research 31 (2001) 767–774

CEMENT AND CONCRETE RESEARCH

Mechanical properties of calcium-leached cement pastes Triaxial stress states and the influence of the pore pressures

F.H. Heukamp*, F.-J. Ulm, J.T. Germaine

Department of Civil and Environmental Engineering, Room I-215, Massachusetts Institute of Technology, 77 Massachusetts Avenue, Cambridge, MA 02139, USA

Received 21 April 2000; accepted 1 February 2001

Abstract

Application of concrete in nuclear waste containments requires knowledge of its mechanical behavior when subjected to calcium leaching. In order to address real-life situations, multiaxial stress states of leached material must be considered. This paper reports results from a series of triaxial tests of calcium-leached cement paste obtained from accelerated leaching tests that operate on an acceleration rate of 300, compared with natural calcium leaching. Along with the global strength loss due to chemical decohesion, an important loss of frictional performance is reported. Environmental scanning electron microscope (ESEM) pictures of both leached and unleached material are presented, and they indicate that this loss of frictional performance can be associated with a highly eroded microstructure perforated by the leaching process. In addition, the frictional behavior of leached cement pastes is found to be strongly dependent on the drainage conditions of the material and thus, on the interstitial pore pressure. Through a poromechanical analysis, it is shown that this high pore pressure sensitivity of leached cement paste can be attributed to the low skeleton-to-fluid bulk modulus ratio, K_s/K_f, of the degraded material, which, together with the increase in porosity, leads to the high compressibility of calcium-leached materials. This low K_s/K_f ratio is the consequence of an *intrinsic* chemical damage of the solid skeleton, which occurs during calcium leaching.

Keywords: Nuclear waste storage; Accelerated calcium leaching; Triaxial testing; Frictional behavior; Chemical damage; Pore pressure; ESEM

1. Introduction

Concrete is commonly employed in radioactive waste disposal as an effective and economical construction material for containment barriers, liners, and encasement of containers. Because of the critical nature of nuclear waste, the load-bearing capacity of concrete containment structures must be ensured over several hundred years. A widely accepted reference scenario for the durability design of waste containers is calcium leaching by pure water [6]. This design scenario refers to the risk of water intrusion in the storage system. It is assumed that the concrete is subjected to leaching by permanently renewed deionized water acting as a solvent. The lower calcium ion concentration in the interstitial pore solution leads to the dissolution of the calcium bound in the skeleton as Portlandite crystals, $Ca(OH)_2$, and calcium-silicate-hydrates (C-S-H) characterized by sharp dissolution fronts [1,8,15]. This calcium leaching leads to a degradation of the mechanical properties of concrete. Moreover, as leaching by deionized water is a very slow process, monitoring the durability of nuclear waste storage structures involves large time scales that complicate experimental assessment.

In terms of chemo-mechanical effects, the loss of elastic stiffness (chemical damage) and the strength loss in uniaxial compression due to calcium leaching have been subject to first studies [7,11,18]. In contrast, little is known about the behavior of leached cementitious materials under bi- or triaxial stress states.

2. Experimental program

The objective of the experiments is to determine the strength domain of leached cementitious materials under triaxial stress states. This requires (1) an accelerated test method able to reproduce in vitro the intrinsic material response that characterizes the long-term behavior of cemen-

* Corresponding author. Tel.: +1-617-253-0251; fax: +1-617-253-6044.

E-mail address: heukamp@mit.edu (F.H. Heukamp).

0008-8846/01/$ – see front matter
PII: S0008-8846(01)00472-0

titious materials, and (2) a homogeneous decalcification state to assess the "real" material response in the mechanical tests.

2.1. Design

Calcium leaching is a coupled diffusion–dissolution process involving sharp dissolution fronts that propagate through the structure. The sharp dissolution fronts are due to the locally quasi-instantaneous dissolution. The time scale of the leaching process is governed by the diffusion properties of the material. Small sample sizes and high calcium efflux favor a rapid leaching process. In the present study, the test program was carried out on pure cement pastes, the basic constituent of concrete, allowing for small and relatively homogeneous material samples. Moreover, the calcium efflux can be artificially accelerated by increasing the chemical equilibrium concentration, i.e. the calcium solubility, at the dissolution front. Leading to a higher calcium concentration gradient in the pore solution, and thus to higher efflux, this can be achieved by replacing the deionized water that is part of the reference scenario by an ammonium nitrate solution (NH_4NO_3). Calculations based on Ref. [3] show that the equilibrium calcium concentration is shifted from ≃22 mmol/l (using deionized water) to ≃2.9 mol/l in a 6-M NH_4NO_3 (480 g/kg) solution.

The dissolution of, e.g. Portlandite [$Ca(OH)_2$] in the ammonium nitrate solution can be written according to the following reaction equation:

$$Ca(OH)_2 + 2NH_4NO_3 \rightleftharpoons Ca^{2+} + 2OH^- + 2H^+ + 2NH_3 + 2NO_3^- \rightleftharpoons Ca(NO_3)_2 + 2NH_{3g} + 2H_2O \quad (1)$$

The dissolution front corresponds to the place where Portlandite is leached. It is the first mineral to be leached; the C-S-H decalcify thereafter [1]. The high solubility of ammonium nitrate (680 g/kg of solution at 20°C), the change to the gaseous phase of NH_3, and the high solubility of calcium nitrate favor the dissolution process. An equilibrium exists between the ammonium (NH_4) and the aqueous ammonia (NH_{3aq}):

$$NH_4^+ \rightleftharpoons NH_{3aq} + H^+; \quad \frac{[NH_{3aq}][H^+]}{NH_4^+} = 10^{-pK_a} \quad (2)$$

where $[NH_{3aq}]$, $[H^+]$, and $[NH_4^+]$ are the activities of the different species. The pH at which the equilibrium concentration of ammonium equals that of ammonia (NH_3) is equal to the pK_a of NH_4^+, 9.25. Hence, for a pH smaller than 9.25, there is always more ammonium than ammonia in solution. During the leaching process, the ammonium in the pore solution of the cementitious material dissociates to ammonia and H^+ [Eq. (2)] due to the basic environment. H^+ reacts with OH^-, reducing the OH^- activity [2], and favoring Portlandite [$Ca(OH)_2$] dissolution. Together with the change to the gaseous phase of NH_3 and the high solubility of calcium nitrate, this qualitatively explains the high calcium equilibrium concentration of ≃2.9 mol/l (6 M NH_4NO_3), which in fine is the key to an accelerated leaching process. In contrast, for pH >9.25, the lack of ammonium reduces the calcium equilibrium concentration and thus, the overall leaching process. This is why it is important to monitor the pH of the aggressive solution during the accelerated leaching experiment. This accelerated leaching has the same characteristics as 'natural' leaching:

- The dissolution that occurs at a higher equilibrium concentration is still quasi-instantaneous in comparison with the diffusion of calcium ions from the dissolution front to the outside, and thus, the leaching process is still governed by the diffusion properties of the material.
- Albeit different in kinetics, the ammonium nitrate-based calcium leaching leads to the same mineral end products in the cementitious material [7].

As a quasi-self-similar diffusion–dissolution problem, the overall acceleration rate can be assessed from the ratio of the similarity parameter of front propagation:

$$a = \left(\frac{\xi_{d1}}{\xi_{d0}}\right)^2 \quad (3)$$

where $\xi_{d0} = x_d/\sqrt{t_0}$ and $\xi_{d1} = x_d/\sqrt{t_1}$ are close to a multiplied constant the self-similar parameters that define the position x_d of the dissolution front in the normal and accelerated leaching setting, respectively (see, e.g. Ref. [15]).

Finally, it has to be mentioned that the maximum solubility of ammonium nitrate in water mentioned above (680 g/kg) shows that more than 6 M ammonium nitrate can be dissolved in water. The calcium equilibrium concentration, in principle, increases with the ammonium nitrate concentration. However, adding ammonium nitrate beyond 6 M does not accelerate the leaching process, due to the limited amount of Portlandite in the cement paste.

2.2. Calcium leaching

The chosen Type I Portland cement (composition, see Table 1) paste samples with a water–cement ratio of w/c = 0.5 are cylinders of diameter 11.5 mm and length 60 mm. After 24 h, the specimens were demoulded and cured in a saturated lime solution for 27 days at 20°C. One-half of the samples was immersed in the 6-M ammonium nitrate solution for accelerated leaching; the other half was stored for control purposes in limewater. To obtain good mixing of the ammonium nitrate solution and most homogeneous leaching conditions possible, the tanks containing the

Table 1
Type I Portland cement constituents, in mass percent

OPC Type I	CaO	SiO_2	Al_2O_3	MgO	SO_3	Na_2O
	62.3	20.8	4.4	3.8	2.9	0.39
	Fe_2O_3	K_2O	C_3Al	C_3S	C_2S	Ignition loss
	2.4	1.28	8	53	20	0.66

Data from producer.

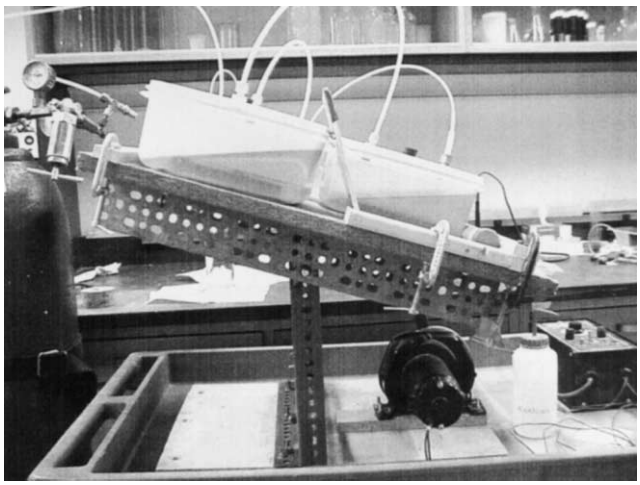

Fig. 1. Oscillating table for controlled calcium leaching.

ammonium nitrate bath were mounted on a slowly oscillating table (Fig. 1). In that way, the bath was constantly agitated, and the sample surfaces were in free contact with the aggressive solution. Each tank of 15×15 cm quadratic shape was filled with 2.2 kg of aggressive solution and contained 26 specimens. In addition, carbonation by CO_2 was prevented through replacing the air in the tanks by pure nitrogen gas (Fig. 1). In parallel, the pH of the solution was monitored. A necessary renewal of the solution due to a lack of ammonium (NH_4^+) would have been indicated by a pH greater than 9.25 [see Eqs. (1) and (2)]. At the chosen combination of ammonium nitrate concentration, bath volume and number of specimens, it turned out that the aggressive solution had not to be renewed during the leaching experiment; the leaching process continuously took place at the highest possible rate. During the leaching process, samples were taken out of the aggressive bath to determine visually the progress of the dissolution front. A square root of time function for the dissolution front progress was obtained being in the order of $\xi_{d1} = 2\ \mathrm{mm}/\sqrt{\mathrm{day}}$ If we take for reference the "natural" progress of the propagation front of $\xi_{d0} = 0.115\ \mathrm{mm}/\sqrt{\mathrm{day}}$ (see, e.g. Ref. [1]), we obtain with the 6-M ammonium nitrate solution (480 g/kg of solution) an overall acceleration of $a = 300$ according to Eq. (3). For the 11.5 mm in diameter cylinder samples, the dissolution front reached the center of the specimens in less than 9 days. However, XRF analysis showed that the average bulk calcium content was still decreasing significantly thereafter (Fig. 2). The quasi-steady state, i.e. homogeneous calcium content, required 45 days of accelerated leaching.

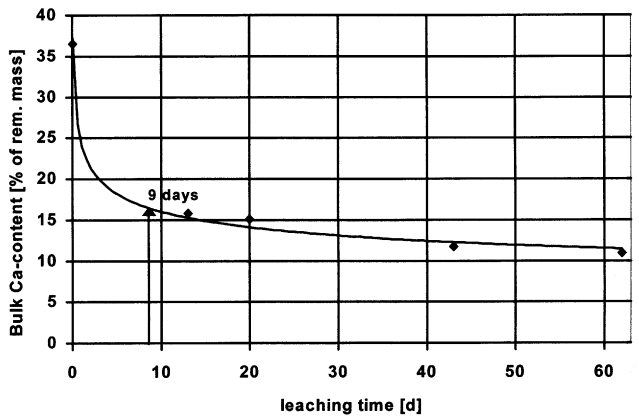

Fig. 2. Bulk calcium content evolution during leaching.

2.3. Triaxial test setup

The triaxial cell used in the experiments has a high-pressure steel chamber. The confinement pressure is applied on the sample that is in a latex membrane by oil. The hydrostatic confinement pressure is applied first before the deviator is added until failure. The displacement rate is constant, and the vertical stress is measured by an internal load cell. Fig. 3 gives a schematic view of the triaxial cell. The test focuses on strength; strains are not of concern.

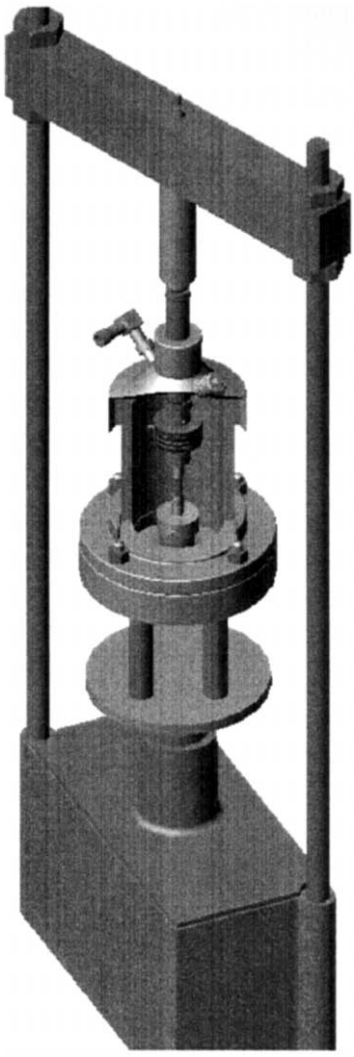

Fig. 3. Schematic view of the triaxial cell.

To avoid the development of expansive calcium nitro-aluminate products [7,14], the degraded samples were kept in the bath until being tested. To have smooth surfaces and parallel ends, the specimens were cut with a diamond saw to a length of 23.5 mm. Confinement pressures up to 10 MPa were applied.

An important issue arises when it comes to triaxial testing of calcium-depleted cement pastes, related to chemical damage, i.e. the irreversible loss of elastic stiffness, due to calcium dissolution. This chemical damage leads to a bulk modulus of the degraded material sample, say 1 GPa [7], which is of the same order as the compressibility modulus of the interstitial solution, i.e. $K_f = 2.3$ GPa. Hence, in contrast to undegraded cementitious materials, the pore pressure in the interstitial space may affect both deformability and strength of the material. To account for this effect, the triaxial tests were carried out under drained and undrained conditions. The drained conditions were assured by a dry filter stone at the base of the specimen.

3. Results

Figs. 4 and 5 show the results of this test campaign in the $\sqrt{3J_2}\times\sigma_m$ stress invariant half-plane. In the triaxial test, the second deviator invariant $\sqrt{J_2}$ and the mean stress σ_m are defined by:

$$\sqrt{J_2} = \sqrt{\frac{1}{2}s_{ij}s_{ij}} = \frac{1}{\sqrt{3}}|\sigma_z - \sigma_r|; \quad \sigma_m = \frac{1}{3}\sigma_{ii} = \frac{1}{3}(\sigma_z + 2\sigma_r) \tag{4}$$

where $s_{ij} = \sigma_{ij} - \sigma_m\delta_{ij}$ is the stress deviator of stress tensor σ_{ij}, and δ_{ij} denotes the Kronecker Delta; σ_z is the vertical stress, and σ_r the radial stress, controlled in the triaxial test

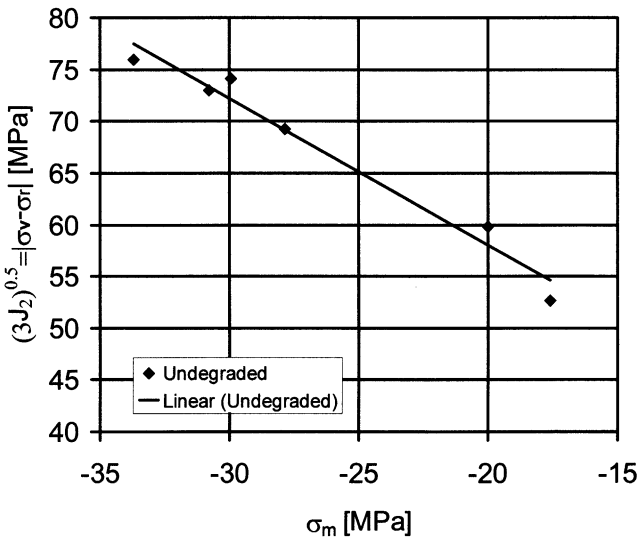

Fig. 4. Unleached paste deviator mean stress plane.

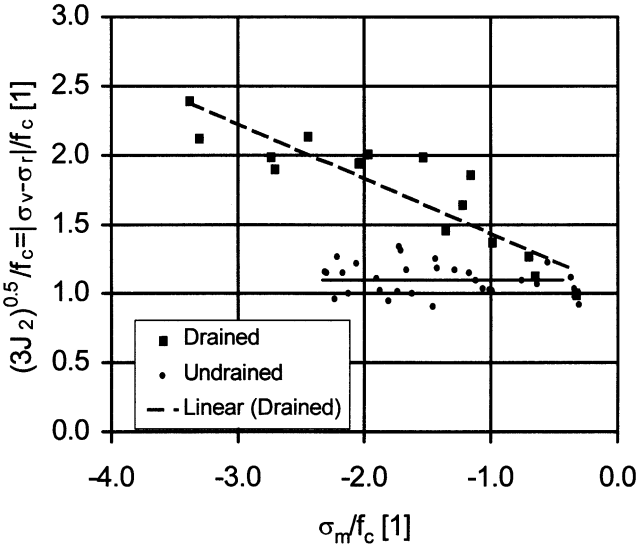

Fig. 5. Degraded paste in normalized deviator mean stress plane (drained and undrained).

setup. The slope $\delta_c = d\sqrt{J_2}/d\sigma_m$ corresponds to the friction coefficient on the compressive stress meridian (see, e.g. Ref. [9]). In Fig. 5, the invariants defined by Eq. (4) are normalized by the uniaxial compression strength obtained on control specimens kept under same chemo-hygral conditions as the tested one. The uniaxial compression strengths for the leached and the unleached paste are summarized in Table 2.

3.1. Unleached cement paste

Fig. 4 shows the well-known frictional behavior of cementitious materials under triaxial stress states (cf. Ref. [20]): Increasing the confinement pressure leads to a significant higher second deviator invariant that the material can support. The friction coefficient that characterizes this property is on the order of $\delta_c = 0.82$.

3.2. Leached cement paste

The leached samples show a more diverse behavior. We note the important overall strength loss related to a chemical decohesion. Both the drained and undrained experiments show this significant strength loss: In uniaxial compression, the chemical decohesion leads to a strength loss of about 90% (see Table 2). In addition, a significant difference in the frictional behavior of drained and undrained samples is observed.

Table 2
Compressive strength f_c, coefficient of variation var, friction coefficient δ_c, and number of tests N

	f_c[MPa]	var[%]	δ_c	N
Unleached	54.1	5.6	0.82	5
Leached	5.1	8.3	0.23	8

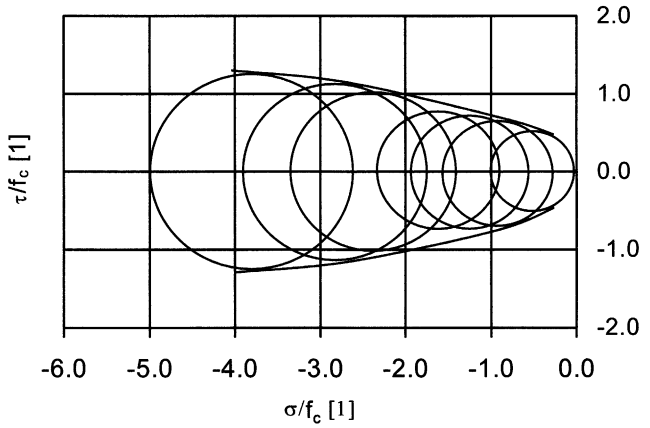

Fig. 6. Leached paste under drained conditions in normalized Mohr stress plane.

3.2.1. Drained experiments

In the drained case (Fig. 5), the linearized friction coefficient is considerably smaller than the one of the undegraded material, in average $\delta_c = 0.23$. Fig. 6 illustrates the drained residual frictional behavior in the Mohr stress plane; the stresses being normalized by the uniaxial compression strength, f_c. The Mohr circles for drained experiments have an increasing diameter with increasing confinement pressure. The envelope with an initially constant slope is flattening at confinement pressures greater than the uniaxial compression strength. The applied confinement pressures go up to twice the uniaxial strength of the degraded material. Similar confinement levels could not be obtained on undegraded samples.

3.2.2. Undrained experiments

Under undrained conditions, no apparent frictional strength enhancement is observed (Fig. 5). This can be ascribed to pore pressure effects. The volumetric strain induced by the externally applied confinement pressure results in pore pressures, which cannot escape in the undrained case. This internal pressure buildup reduces the 'effective' confinement stress of the skeleton, which therefore, cannot mobilize friction in the material during deviator loading. In the Mohr stress plane, this behavior translates into circles of nearly constant diameter (Fig. 7). The constant second deviator invariant for different confinement levels suggests that the pore pressures are of the order of magnitude of the applied confinement pressure, that is up to 10 MPa.

4. Discussion and analysis

4.1. Environmental scanning electron microscope (ESEM) analysis

Figs. 8 and 9 show the microstructure of degraded and the undegraded microstructure of the cement paste obtained with an ESEM at a magnification varying between 300 and 10,000. In contrast to other microscope techniques, e.g. SEM, an ESEM can be operated with wet samples, avoiding cracking due to drying. The material surfaces shown in Figs. 8 and 9 are freshly fractured and nitrogen-cleaned.

The pictures indicate that the significant chemically induced loss of frictional performance can be attributed to a highly eroded microstructure perforated by calcium leaching.

- While the microstructure of the unleached cement paste remains compact throughout the different scales, the leached material appears discontinuous already at a magnification of 300 (Fig. 8A1). In comparison to the undegraded paste (Fig. 8A2), the microstructure of the leached material is perforated in a regular manner by large pores. In the 1000 magnification, this porotic microstructure shows a cauliflower-like structure (Fig. 8B1), perforated by pores of the same size as the solid skeleton walls.
- Details of the cauliflower structure, in a 5000 magnification (Fig. 9A1) and a 10,000 magnification (Fig. 9B1) show the remnants of an initially highly heterogeneous and disordered microstructure (Figs. 9A2 and B2). Smooth plated solid remnants are separated by large pores, which become the main part of the pictures. The pore size at this scale may be attributed to the dissolution of Portlandite crystals, which are the first to dissolve during calcium leaching, followed by the C-S-H decalcification. The remaining C-S-H sheets have a characteristic size 10–100 times smaller than the one of Portlandite [12,17]. The friction that is mobilized during deviator loading in sane materials at the Portlandite crystal interfaces and in the highly heterogeneous compact microstructure is strongly reduced. Under triaxial loading of degraded materials, the remaining solid walls break and collapse without much frictional interaction with neighboring solid walls. Consequently, the stabilizing effect of a hydrostatic confinement on the overall shear resistance is reduced, leading to the observed chemical-induced loss of frictional performance.

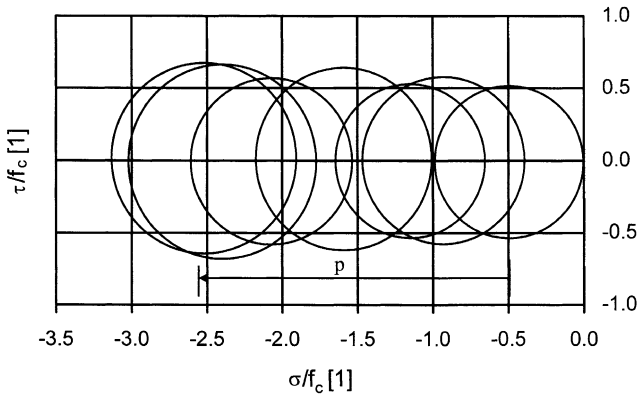

Fig. 7. Leached paste under undrained conditions in normalized Mohr stress plane.

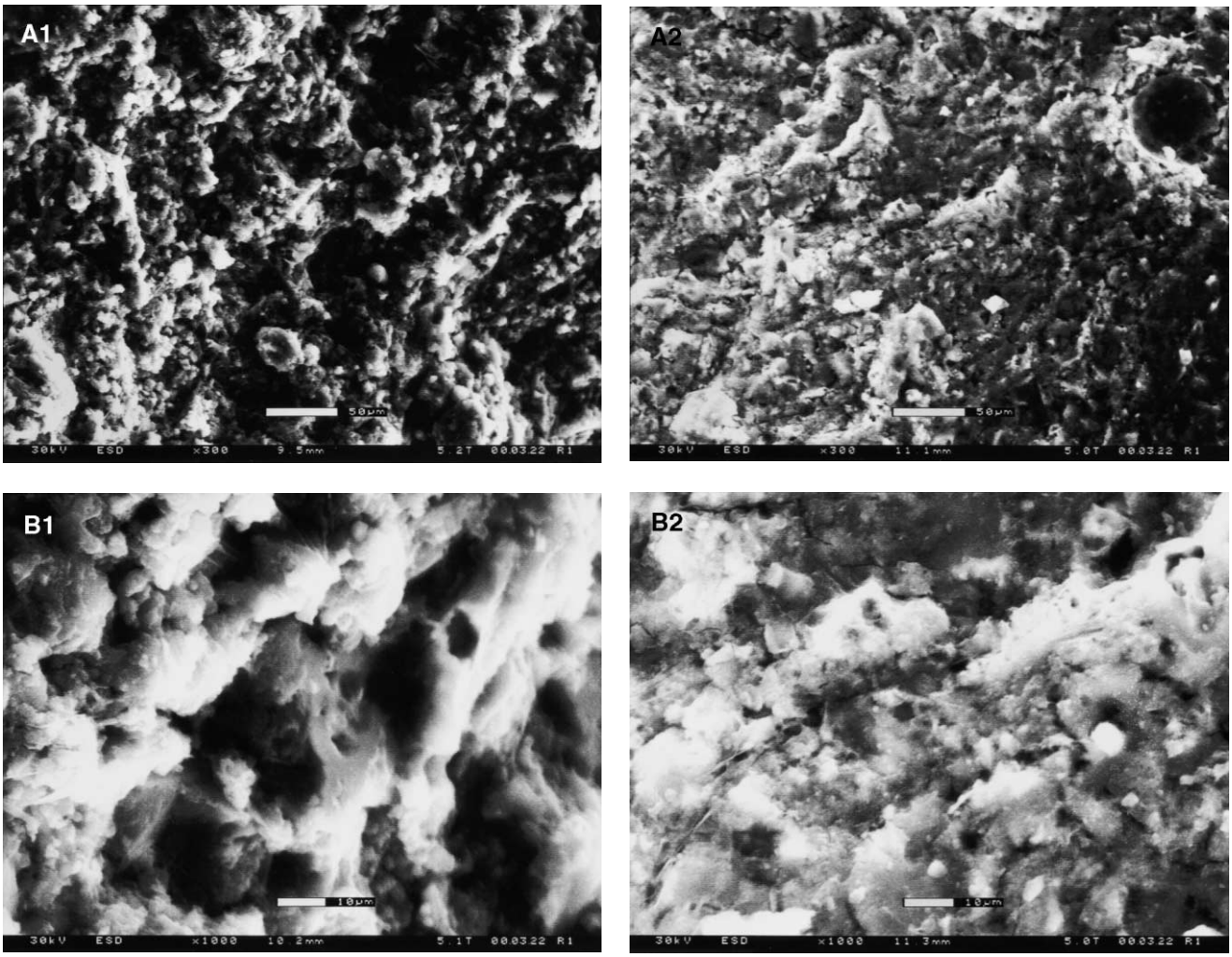

Fig. 8. ESEM picture of leached and unleached paste. Magnification 300 and 1000. A1: Leached paste, Mag.: 300. A2: Unleached paste, Mag.: 300. B1: Leached paste, Mag.: 1000. B2: Unleached paste, Mag.: 1000.

4.2. Pore pressure sensitivity

The reported difference in the drained and undrained behavior of leached cement paste indicates a nonnegligible role of the pore pressure on both deformability and strength domain of the material, but they were not measured in the experiments. This pressure sensitivity may be attributed to the increased porosity of the degraded material, but also to the chemical damage of the solid skeleton, as shown in the ESEM pictures. Our argument is a poromechanical one. During elastic loading, cement paste can be considered as an isotropic saturated porous material. Within the framework of the Biot–Coussy theory of poromechanics, the mean stress $\sigma_m = 1/3\sigma_{ii}$, and the pore pressure p are related to volume strain $\epsilon = \varepsilon_{ii}$ and the relative change in fluid mass v_f by (e.g. Ref. [10]):

$$\begin{cases} \sigma_m = K_0\epsilon - bp \\ p = M(-b\epsilon + v_f) \end{cases} \tag{5}$$

K_0, b, and M denote the drained bulk modulus, the Biot coefficient, and the Biot modulus. The coefficients b and M can be assessed from:

$$b = 1 - \frac{K_0}{K_s}; \quad \frac{1}{M} = \frac{b-\phi_0}{K_s} + \frac{\phi_0}{K_f} \tag{6}$$

with ϕ_0 the initial porosity of the material, K_f the bulk modulus of the fluid, and K_s the bulk modulus of the skeleton. The skeleton bulk modulus K_s can be estimated from the homogenization theory that Kendall et al. [13] applied to the Young's modulus of porous materials:

$$K_0 = K_s(1-\phi_0)^3 \tag{7}$$

In the case of an undrained experiment, for which the fluid mass variation is zero, $v_f = 0$, Eqs. (5)–(7) give [Eq. (8)]:

$$\frac{1}{B} = -\left(\frac{\sigma_m}{p}\right) = \frac{K_0}{Mb} + b = 1 - \left(1 - \frac{K_s}{K_f}\right)\frac{\phi_0(1-\phi_0)^3}{1-(1-\phi_0)^3} \tag{8}$$

$B = -p/\sigma_m$ is often referred to as compressibility coefficient or Skempton factor [4,5,16]: It quantifies the amount of the macroscopically applied stress σ_m, which is carried in an

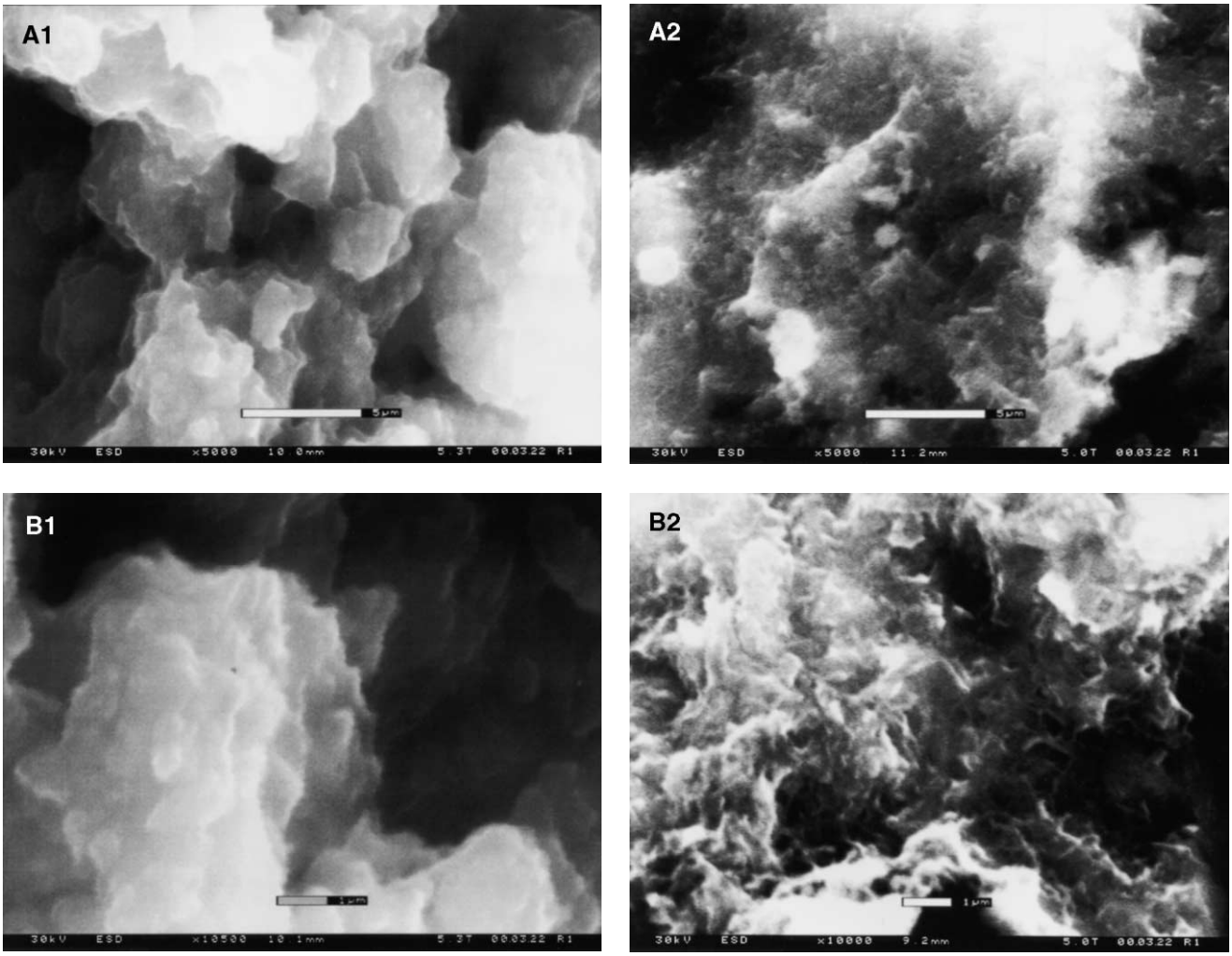

Fig. 9. ESEM picture of leached and unleached paste. Magnification 5000 and 1000. A1: Leached paste, Mag.: 5000. A2: Unleached paste, Mag.:5000. B1: Leached paste, Mag.: 10500. B2: Leached paste, Mag.: 10000.

undrained test by the saturating fluid pressure. Fig. 10 shows this function for two different K_s/K_f ratios. The lower value, $K_s/K_f = 3$, corresponds roughly to the value of a degraded sample; the upper value $K_s/K_f = 20$, to the one of the sane cement paste. The figure shows the two parameters, which govern the pressure sensitivity of cementitious materials: the porosity ϕ_0 and the skeleton-to-fluid bulk modulus ratio K_s/K_f. The lower the K_s/K_f ratio, the less sensitive is the function $-p/\sigma_m$ to a change in initial porosity. This shows that the dominating parameter governing the pressure sensitivity of degraded cementitious materials is the K_s/K_f ratio, associated with an *intrinsic* chemical damage of the solid part of the eroded porotic microstructure (Fig. 9A1 and B1). For a typical value of the initial porosity of the degraded material of $\phi_0 = 0.5$, the part of the total applied stress taken over by the pore pressure is on the order of $-p/\sigma_m = 90\%$. This means that the "effective" confinement stress $\sigma_m' = \sigma_m + bp = 0.1\sigma_m$ in an undrained test, to which the chemically eroded skeleton is

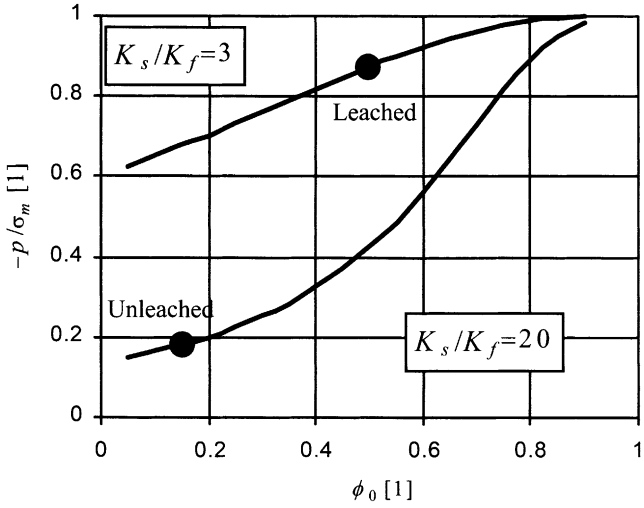

Fig. 10. Skempton coefficient B as a function of the initial porosity ϕ_0 and the K_s/K_f ratio.

subjected, is small. In the Mohr stress plane (Fig. 7), all the tests at different confinement pressure levels are, in terms of effective stress, only one triaxial test equivalent to the uniaxial compression test. In return, $-p/\sigma_m \leq \phi_0 \backsimeq 0.2$ for the undegraded material, and shows that the pore pressures that develop in the highly disordered compact cementitious microstructure (Fig. 9A2 and B2) are small in comparison to the hydrostatic stress mobilizing the frictional behavior.

5. Conclusion

(1) The paper deals with triaxial mechanical behavior of calcium-leached cement paste, to which little attention was paid in the past. The triaxial behavior of leached cement paste is characterized by an important overall strength loss, a loss in frictional performance, and a high sensitivity to drained and undrained conditions. The linearized friction coefficient (compressive meridian) decreases from $\delta_c = 0.82$ to $\delta_c = 0.23$ in the drained case. In the undrained case, due to the internal pressure buildup, no apparent frictional behavior is observed.

(2) The low frictional coefficient and the high sensitivity of degraded cement pastes to drained and undrained conditions can be attributed to a craggy and highly perforated microstructure, and shows some striking similarity with the behavior of clays. This similarity may be attributed to the level of the solid skeleton to the similar structure of C-S-H and clay platelets, as recently reported by Viallis et al. [19].

(3) The importance of the pore pressures on the ultimate frictional behavior of chemically degraded cementitious materials is critical. It can be attributed to the low skeleton-to-fluid bulk modulus ratio K_s/K_f, and thus, to the chemical damage of the solid constituent. This pressure sensitivity should be considered in design and operation of secure applications of concrete in nuclear waste storage, as many possible stress situations may occur under (almost) undrained conditions.

(4) The obtained results show the importance of "Thinking 3D" when monitoring the durability performance of concrete in nuclear waste containment is at stake. Additional material tests on mortars and concrete are necessary to complete the results for other meridians than the compressive meridian considered in this paper, and to generalize the behavior for two solid phase cementitious materials.

Acknowledgments

This research was performed as part of Grant No. DE-FG03-99SF21891/A000 of the US Department of Energy (DOE). The authors gratefully acknowledge the support for this work by the Nuclear Energy Research Initiative Program of DOE. This research also benefited from collaboration with the C.E.A., Saclay, France, through Dr. J. Sercombe. We thank Professor B. Völker of the MIT Civil and Environmental Engineering Department for fruitful discussions and helpful comments about the chemical aspects of this paper.

References

[1] F. Adenot, M. Buil, Modelling of the corrosion of the cement by deionized water, Cem. Concr. Res. 22 (4) (1992) 451–457.
[2] F. Adenot, B. Gérard, J.M. Torrenti, Etat de l'art, in: J.P. Olivier, J.M. Torrenti, O. Didry, F. Plas (Eds.), La Dégradation des Bétons, Communications en Mécanique, Hermes, Paris, 1999, pp. 19–46.
[3] U.R. Berner, Modelling the incongruent dissolution of hydrated cement minerals, Radiochim. Acta 44–45 (1988) 387–393.
[4] A.W. Bishop, The influence of an undrained change in stress on the pore pressure in porous media of low compressibility, Geotechnique 23 (3) (1973) 435–442.
[5] A.W. Bishop, D.W. Hight, The value of poisson's ratio in saturated soils and rocks stressed under undrained conditions, Geotechnique 27 (3) (1977) 369–384.
[6] M. Buil, E. Revertegat, J. Oliver, Modeling cement attack by pure water, Int. Symp. on Stabilization/Solidification of Hazardous, Radioactive and Mixed Wastes, Williamsburg, 1990.
[7] C. Carde, R. Francois, Effect of the leaching of calcium hydroxide from cement paste on mechanical and physical properties, Cem. Concr. Res. 27 (4) (1997) 539–550.
[8] C. Carde, R. Francois, J.M. Torrenti, Leaching of both calcium hydroxide and C-S-H from cement paste: Modeling the mechanical behavior, Cem. Concr. Res. 26 (8) (1996) 1257–1268.
[9] W.F. Chen, D.J. Han, Plasticity for Structural Engineers, Springer, New York, 1988.
[10] O. Coussy, Mechanics of Porous Continua, Wiley, Chichester, 1995.
[11] B. Gérard, Contribution des couplages mécanique–chimie–transfert dans la tenue à long terme des ouvrages de stockage des déchets radioactifs. PhD dissertation, ENS Cachan, France, 1996. (in French).
[12] I. Jawed, J. Skalny, J.F. Young, Hydration of portland cement, in: P. Barnes (Ed.), Structure and Performance of Cements, Applied Science Publishers, London, 1983, pp. 237–318.
[13] K. Kendall, A.J. Howard, J.D. Birchall, The relation between porosity, microstructure and strength, and the approach to cement-based materials, Philos. Trans. R. Soc. London, Ser. A 310 (1983) 139–153.
[14] F.M. Lea, The action of ammonium nitrate salts on concrete, Mag. Concr. Res. 17 (52) (1965) 115–116.
[15] M. Mainguy, O. Coussy, Propagation fronts during calcium leaching and chloride penetration, ASCE J. Eng. Mech. Div. 126 (3) (2000) 250–257.
[16] A.W. Skempton, The pore-pressure coefficients A and B, Geotechnique 4 (1954) 143–147.
[17] H.F.W. Taylor, Cement Chemistry, second ed., Thomas Telford, London, 1997.
[18] F.J. Ulm, J.M. Torrenti, F. Adenot, Chemoporoplasticity of calcium leaching in concrete, ASCE J. Eng. Mech. Div. 125 (10) (1999) 1200–1211.
[19] H. Viallis, P. Faucon, J.C. Petit, J. Virlet, A. Nonat, Analogy between calcium silicate hydrates and clays: Study of cation fixation at the C-S-H surface, In: Sixth Conference and Exhibition of the European Ceramic Society. (number 60, British Ceramic Proceedings), 1999, pp. 271–272, June.
[20] T. von Karman, Festigkeitsversuche unter allseitigem Druck, Z. Ver. Dtsch. Ing. 2 (55) (1911) 1749–1758.